Magnetic-field-induced birefringence in a homeotropic ferronematic liquid-crystal wedge

Shu-Hsia Chen and C. W. Yang

Institute of Electro-Optical Engineering, National Chiao Tung University, Hsinchu, Taiwan 30050, China

Received March 8, 1989; revised manuscript received May 3, 1990; accepted July 16, 1990

The magnetic-field-induced birefringence in wedged homeotropic ferronematic liquid crystals is studied. Theoretical results for small distortions are obtained in terms of the elastic continuum theory of liquid crystals. The results of birefringence measurements are in good agreement with the predictions of the theory.

From studies of the effect of an external magnetic field on liquid crystals (LC's), it is well known that a strong magnetic field[1] is required because the anisotropic part of the diamagnetic susceptibility ($\Delta\chi$) of the LC is rather small.[2] To obtain the magnetically induced birefringence in LC's at practical field strengths, ferromagnetic gains[1,3–10] have been used. Thus, from practical considerations, it is natural to study the physical properties of ferronematic crystals,[6] which are magnetically doped nematic LC's. In our previous research[6,7,9,10] the magnetically induced birefringence in a homeotropic ferronematic crystal packed in two parallel plates of glasses was studied. However, wedge LC films show interesting properties. For example, Grover[11] reported that the initial bend in the molecular alignment of a homeotropic nematic wedge causes a relaxation in the reorientational degeneracy of the electrically induced Freedericksz transition. A new type of domain, occurring in twisted-wedge nematic structures, was reported by Martin-Pereda *et al.*[12] Furthermore, several LC-based optical devices that use different configurations and electric, magnetic, or optical external fields have been proposed.[13–17] With its thickness gradient configuration, the wedge LC cell has high potential for optical devices. However, to our knowledge, no report exists on the magneto-optic effect of a wedge LC film. The low field requirement for ferronematic LC's makes experiments on the magneto-optic effect easy. In this Letter the magnetic-field-induced birefringence for a homeotropic ferronematic wedge in the low-field regime is reported. The experimental results agree with theoretical predictions based on the elastic continuum theory of LC's.

Consider a homeotropically aligned wedged film of ferronematic LC (FNLC) as shown in Fig. 1. The wedge has an angle $\alpha \approx 1°$ with a 350-μm spacer placed 2 cm from the apex. For a small α, the unperturbed director makes an angle $\theta_0 = \alpha Z/D$ with the Z axis, where D is the thickness of the wedge at that point measured on the Z axis. The magnetization vector M, which is always perpendicular to the director n, points either inward or outward with respect to the contacting edge of the wedge. After a vertical magnetic field H is applied, four different configurations can occur, as shown in Fig. 2. The configuration shown in Fig. 1(c) corresponds to Figs. 2(a) and 2(b). In the low-field regime, the distortion is weak, and one may neglect the dependence of the orientational angle on the x coordinate since α is small. We define the orientational angle θ of the director $\mathbf{n}$ as $\theta(H, Z) = (\alpha/D)Z + \theta_r(H, Z)$, where θ_r indicates the field-induced reorientation angle.

To find the magnetic-field-induced birefringence of the film, we must know the molecular reorientation angle θ_r. By using the elastic continuum theory, this can be obtained by minimizing the total free energy per unit wall area. This energy is given by

$$f = \int_0^D \left[\frac{1}{2}\left(\frac{\partial\theta}{\partial Z}\right)^2 K_{33}(1 + K\sin^2\theta) \mp MH\sin\theta\right]\mathrm{d}Z, \tag{1}$$

where the upper sign is for H up and the lower sign is for H down and $K = (K_{11} - K_{33})/K_{33}$, with K_{11} and K_{33} the splay and bend elastic constants, respectively. By minimizing Eq. (1) with the Euler–Lagrange equation, one can readily show that

$$\frac{\mathrm{d}^2\theta_r}{\mathrm{d}Z^2} \mp \frac{MH}{K_{33}}\left[\sin\left(\frac{\alpha}{D}Z\right)\theta_r - \cos\left(\frac{\alpha}{D}Z\right)\right] = 0. \tag{2}$$

When we solve Eq. (2) by the power-series method and take the boundary conditions $\theta_r(Z = \pm D/2) = 0$, then

$$\theta_r(H, Z) = \pm\frac{DB}{2}\left[Z + \sum_{n=1}^{\infty}\frac{(\pm 1)^n A^n Z^{3n+1}}{\prod_{m=1}^{n}(3m)(3m+1)}\right] + C\sum_{n=1}^{\infty}\frac{(\pm 1)^n A^{n-1} Z^{3n+1}}{\prod_{m=1}^{n}(3m)(3m+1)} \mp \frac{B}{2}\left[Z^2 + \sum_{n=1}^{\infty}\frac{(\pm 1)^n A^n Z^{3n+2}}{\prod_{m=1}^{n}(3m+1)(3m+2)}\right], \tag{3}$$

0146-9592/90/191049-03$2.00/0

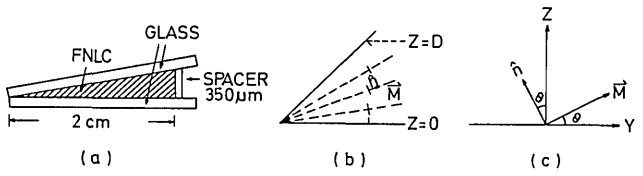

Fig. 1. Sample geometry.

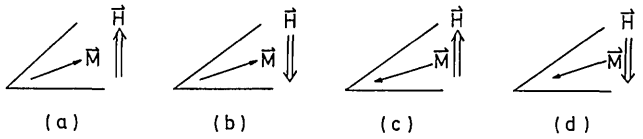

Fig. 2. Sample magnetization configurations.

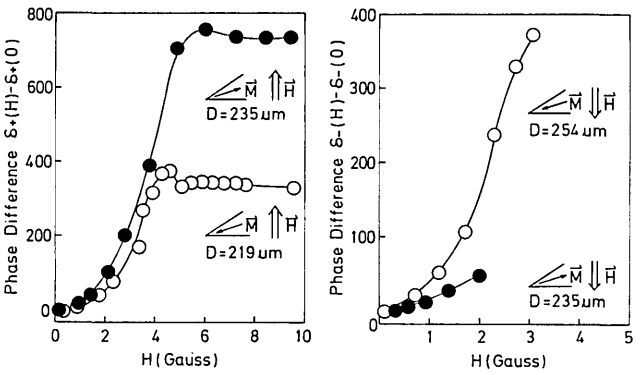

Fig. 3. Magnetic-field-induced birefringence.

where $A = MH\alpha/(K_{33}D)$, $B = MH/K_{33}$, and $C = MH\alpha^2/(2K_{33}D^2)$. For small distortion and neglecting higher-order terms, we have

$$\theta(Z, H) = \frac{\alpha}{D} Z \pm \frac{B}{2} Z(D - Z). \tag{4}$$

The magnetic-field-induced molecular reorientation can be found by measuring the corresponding induced change in birefringence. For a probe beam propagating along the Z axis, the phase retardation is given by

$$\delta_{\pm} = \frac{2\pi}{\lambda}(n_e - n_o)\left(\frac{1}{3}\alpha^2 D \pm \frac{1}{12}\alpha B D^3 + \frac{1}{120} B^2 D^5\right), \tag{5}$$

where n_e and n_o are the extraordinary and ordinary indices of refraction of the LC, respectively, and λ is the wavelength of the probe beam. For convenience, we define

$$\Delta\delta_1 = \left[\delta_+ + \delta_- - \frac{2\pi}{\lambda}(n_e - n_o) - \frac{2}{3} D\alpha^2\right]$$

$$= \frac{2\pi}{\lambda}(n_e - n_o)\frac{1}{60} B^2 D^5, \tag{6}$$

$$\Delta\delta_2 = \delta_+ - \delta_- = \frac{2\pi}{\lambda}(n_e - n_o)\frac{1}{6}\alpha B D^3. \tag{7}$$

These two equations also hold true for the cases shown in Figs. 2(c) and 2(d), where B has a negative value.

In our experiment, the ferronematic LC is magnetically doped *N-P*-methoxybenzylidene-*p*-butylaniline[6] with a volume filling factor of 1.71×10^{-5}. The magnetic particles are γ-Fe_2O_3 needles 0.5 μm long and have an aspect ratio of ~7:1, a density of 4.78 g/cm^3, and a saturation magnetization of 338.4 ergs/G-cm^3. Their magnetic dipole moments point along the long axes of the particles. These needles are coated with dimethyl octadecyl aminopropyl trimethoxysilyl chloride (DMOAP) to prevent clumping. The sample film is made by sandwiching the ferronematic LC between two glass plates. The wedge is achieved by using a 350-μm spacer, as shown in Fig. 1(a). The glass plates are coated with DMOAP for homeotropic alignment.

The sample was examined by microscopy and conoscopy. The field-induced birefringence was mea-

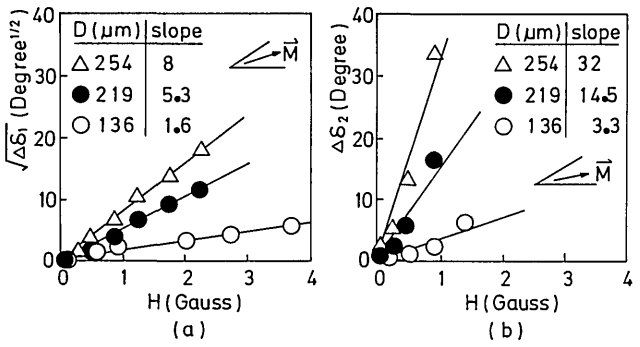

Fig. 4. Phase difference versus the field strength for M pointing outward.

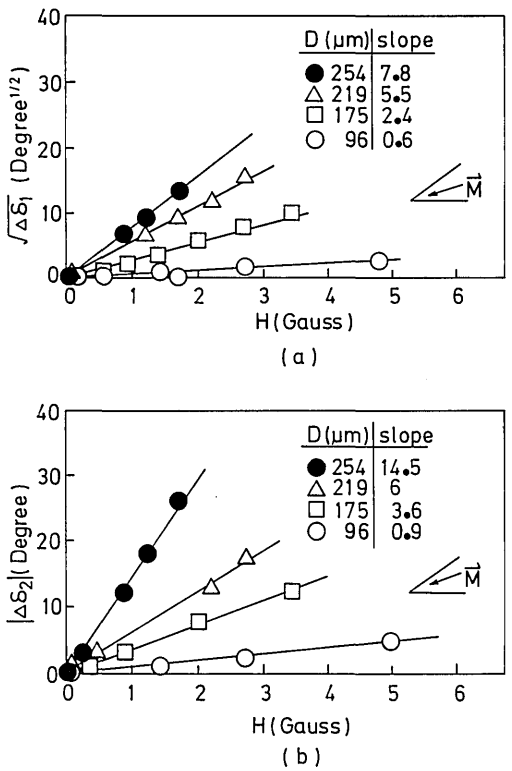

Fig. 5. Phase difference versus the field strength for M pointing inward.

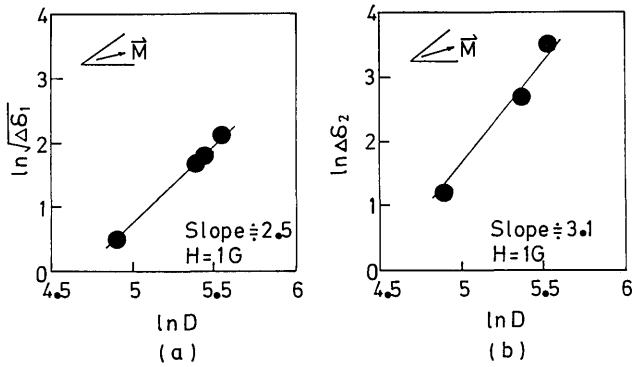

Fig. 6. Phase difference versus the sample thickness for M pointing outward.

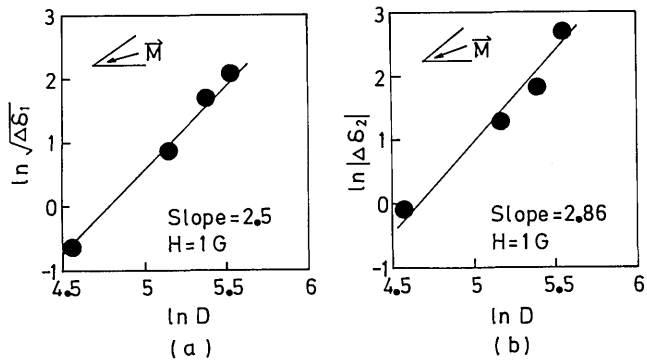

Fig. 7. Phase difference versus the sample thickness for M pointing inward.

sured with a He–Ne placed laser.[6] During the measurement the sample film was placed horizontally. The magnetic dipole moment of the ferronematic matrix is initially aligned by the horizontal component of the Earth's field. A magnetic field is applied vertically with a pair of Helmholtz coils. The induced phase difference is measured first for H upward and then for H downward. These two are then added or subtracted to obtain $\Delta\delta_1$ or $\Delta\delta_2$ from Eq. (6) or (7), respectively.

Some typical phase measurements are shown in Fig. 3 for different sample configurations. Figure 3(a) shows the magnetic field strength (H) dependence of the phase change, $\delta_+(H) - \delta_+(0)$. Figure 3(b) shows the phase change, $\delta_-(H) - \delta_-(0)$, versus H. The field dependence of the square root of $\Delta\delta_1$ and the field dependence $\Delta\delta_2$ for the small-field regime are shown in Figs. 4 and 5, respectively. The data in the figures exhibit the linear relationships between the phase and the magnetic field strength that are predicted by Eqs. (6) and (7). In high magnetic fields, the magnetic grains flocculate into clumps as is expected.

In Figs. 6(a) and 7(a), $\ln\sqrt{\Delta\delta_1}$ is plotted versus $\ln D$ from the data in Figs. 4(a) and 5(a), respectively, with a fixed magnetic field strength (H = 1 G). The slopes are found to be 2.5 for both cases. This indicates that $\Delta\delta_1$ is proportional to the fifth power of the thickness of the nematic matrix as predicted by Eq. (6). Equation (7) predicts that $\Delta\delta_2 \propto D^3$; as shown in Figs. 6(b) and 7(b), $\Delta\delta_2$ is indeed proportional to the cube of the sample thickness D.

In conclusion, in the low magnetic field regime, the continuum theory predicts that $\Delta\delta_1$ is proportional to the square of H and the fifth power of D and that $\Delta\delta_2$ is proportional to H and the cube of D. The birefringence measurement results are in good agreement with these predictions.

References

1. F. Brochard and P. G. de Gennes, J. Phys. **31,** 691 (1970).
2. P. G. de Gennes, *The Physics of Liquid Crystals* (Clarendon, Oxford, 1974).
3. J. Rault, P. E. Cladis, and J. P. Burger, Phys. Lett. **32A,** 199 (1970).
4. L. Liebert and A. Martinet, J. Phys. (Paris) Lett. **40,** L-363 (1979).
5. C. F. Hayes, Mol. Cryst. Liq. Cryst. **36,** 245 (1976).
6. S. H. Chen and N. M. Amer, Phys. Rev. Lett. **51,** 2298 (1983).
7. S. H. Chen and S. H. Chiang, Mol. Cryst. Liq. Cryst. **144,** 359 (1987).
8. A. M. F. Neto and M. M. F. Saba, Phys. Rev. A **34,** 3483 (1986).
9. S. H. Chen and B. J. Liang, Opt. Lett. **13,** 716 (1988).
10. Yu. L. Raikher, S. V. Burylov, and A. N. Zakhlevnykh, Sov. Phys. JETP **64,** 319 (1986).
11. C. P. Grover, Mol. Cryst. Liq. Cryst. **127,** 331 (1985).
12. J. A. Martin-Pereda, M. A. Muriel, and J. M. Oton, Appl. Opt. **23,** 2159 (1984).
13. I. C. Khoo and S. L. Zhuang, Appl. Phys. Lett. **37,** 3 (1980).
14. M. A. Muriel and J. A. Martin-Pereda, J. Opt. Soc. Am. **70,** 1610 (1980).
15. J. A. Martin-Pereda and M. A. Muriel, Europhys. Conf. Abstr. **4I,** L2 (1980).
16. J. A. Martin-Pereda and M. A. Muriel, presented at Electrooptics/Lasers 80 Meeting, 1980.
17. J. A. Martin-Pereda and F. L. Lopez, Opt. Lett. **7,** 590 (1982).